
Faculty of Science

Faculty Publications

This is a post-print version of the following article:

Photochemical behavior of biosupramolecular assemblies of photosensitizers, cucurbit[*n*]urils and albumins

Javiera Caceres, Jose Robinson-Duggon, Anita Tapia, Constanza Paiva, Matias Gomez, Cornelia Bohne & Denis Fuentealba

December 2016

The final publication is available via Royal Society of Chemistry at:

<https://doi.org/10.1039/C6CP07749H>

Citation for this paper:

Caceres, J., Robinson-Duggon, J., Tapia, A., Paiva, C., Gomez, M., Bohne, C., & Fuentealba, D. (2016). Photochemical behavior of biosupramolecular assemblies of photosensitizers, cucurbit[*n*]urils and albumins. *Physical Chemistry Chemical Physics*, 19, 2574-2582. <https://doi.org/10.1039/C6CP07749H>.

Photochemical Behavior of Biosupramolecular Assemblies of Photosensitizers, Cucurbit[*n*]uril and Albumin

Javiera Cáceres^a, José Robinson-Duggon^a, Anita Tapia^a, Constanza Paiva^a, Matías Gómez^a, Cornelia Bohne^b and Denis Fuentealba^{a*}

Received 00th January 20xx,
Accepted 00th January 20xx

DOI: 10.1039/x0xx00000x

www.rsc.org/

Biosupramolecular assemblies combining cucurbit[*n*]urils (CB[*n*]s) and proteins for the targeted delivery of drugs has the potential to improve the photoactivity of photosensitizers used in the photodynamic therapy of cancer. Understanding the complexity of these systems and how it affects the properties of photosensitizers is the focus of this work. We used acridine orange (AO⁺) as a model photosensitizer and compared it with methylene blue (MB⁺) and a cationic porphyrin (TMPyP⁴⁺). Encapsulation of the photosensitizer into CB[*n*]s (*n* = 7,8) modified their photoactivity. In particular for AO⁺ the photo-oxidation of HSA was enhanced in the presence of CB[7], meanwhile it was decreased when included into CB[8]. Accordingly, peroxide generation and protein fragmentation were also increased when AO⁺ was encapsulated into CB[7]. The triplet excited state lifetimes of all the photosensitizers were lengthened by their encapsulation into CB[*n*]s, while the singlet oxygen quantum yield was enhanced only for AO⁺ and TMPyP⁴⁺, being decreased for MB⁺. The results obtained in this work prompt the necessity of further investigating this kind of hybrid assemblies as drug delivery systems because of their possible applications in biomedicine.

Introduction

The high costs of drug discovery and development, and the extensive times needed for approval impose a big economical challenge for the pharmaceutical industry over the next decades.¹ One plausible strategy to overcome this issue is potentiating drugs that already exist and/or tailoring them for the treatments of specific diseases, which can be done with drug delivery systems (DDSs).²⁻⁵ DDSs not only have the potential to improve drug transport, but can also help to control the release of the drug and to target specific tissues such as cancer,⁶ which continues to demand important development efforts for better prognosis.¹

One promising treatment for several types of cancer is photodynamic therapy (PDT), which is based on the action of light on a photoactive drug (photosensitizer), which in the presence of oxygen induces cytotoxicity due to the generation of reactive oxygen species (ROS).⁷⁻¹⁰ This is an area of research where the delivery system can play an essential role to improve biodistribution and tumor accumulation.⁸ Many vehicles have been proposed to deliver payloads of drugs such

as nanoparticles, quantum dots, proteins, macrocycles, polymers and liposomes, among others.¹¹ Recent work on DDSs involving photoactive drugs include polymeric nanoparticles,¹²⁻¹⁵ calcium carbonate microparticles,¹⁶ graphene oxide nanosheets,¹⁷ photo-responsive nanocarriers,^{18, 19} and novel optical fibers which can deliver both the photoactive drug and/or only singlet oxygen.²⁰⁻²² In spite of the many varieties of DDSs being studied, few of them are being marketed to date.⁶

Albumin conjugates have been investigated extensively as drug carriers over the last decade,²³⁻²⁵ and constitute one of the examples of DDSs that have effectively reached the public.^{6, 25} Albumins are natural fatty acid carriers thanks to their multiple hydrophobic binding sites,^{26, 27} a property that is favorable for the transport of many drugs.^{28, 29} The albumin's long circulation times in the bloodstream, small size, lack of immunogenicity and great stability render it ideal for drug delivery applications.^{6, 11, 23-25} Additionally, albumins can penetrate the defective vascularity of tumors and be retained.⁶ In spite of these advantages, when it comes to photoactive drugs, albumins modify the photochemistry of the drugs,^{30, 31} and often reduce the action of photosensitizers.³²⁻³⁵ Moreover, there is no general strategy to release drugs from albumins.

On the other hand, cucurbit[*n*]urils (CB[*n*]s) have recently emerged as potential candidates for drug delivery due to their ability to bind several types of drugs.³⁶⁻³⁸ Although not yet approved for use, CB[*n*]s are expected to follow cyclodextrins in the near future.^{11, 39} Unlike cyclodextrins, binding to CB[*n*]s is extremely high for a synthetic macrocycle, reaching binding constants higher than 10¹⁵ M⁻¹.^{40, 41} CB[*n*]s have been shown to

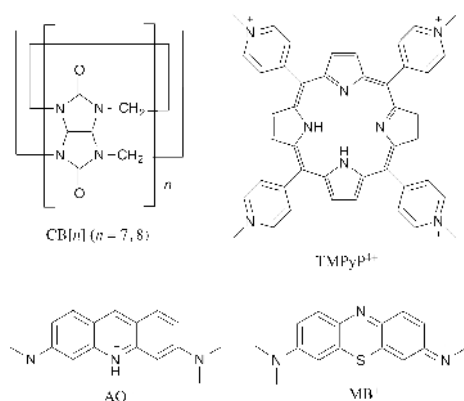
^a Laboratorio de Estructuras Biosupramoleculares, Departamento de Química Física, Facultad de Química, Pontificia Universidad Católica de Chile, Santiago, Chile. E-mail: dlfuente@uc.cl

^b Department of Chemistry, University of Victoria, P.O. Box 1700 STN CSC, Victoria, BC, Canada V8W 2Y2.

Electronic Supplementary Information (ESI) available: Absorption spectra for AO⁺ species during irradiation in the presence of HSA, HSA photo-oxidation mediated by MB⁺@CB[7] complex in D₂O, and singlet oxygen detection by ABMA. See DOI: 10.1039/x0xx00000x

be non-toxic,⁴²⁻⁴⁴ they are able to cross the cell membrane,⁴⁵ and are highly soluble in biological fluids.³⁷ One important advantage of CB[n]s over proteins is that drug release is easily controlled by competitive host-guest chemistry.^{40, 46-49}

The combination of the properties of albumins and CB[n]s in one *biosupramolecular* drug delivery vehicle could be of much benefit for the field. This kind of architecture was first reported by W. Nau, A. C. Bhasikuttan and co-workers for the brilliant green, CB[7] and bovine serum albumin (BSA) complex.⁵⁰ Later work by X. Wang and collaborators reported on the interaction of the well-known photosensitizer tetra(1-methylpyridinium)porphyrin (TMPyP⁴⁺) with CB[8] and BSA,⁵¹ opening a new scope for the use of CB[n]s in PDT applications. Such ternary complexes are very scarce in the literature and their applications are therefore limited. We recently reported on the interaction of another well-known photosensitizer acridine orange (AO⁺) with CB[7] and human serum albumin (HSA), and found no such interaction with the protein in the presence of CB[8].⁵² The latter is an interesting model system in the first place because AO⁺ is active as a PDT agent *in vivo*,^{53, 54} and this molecule forms complexes with either HSA, CB[7] or CB[8], and simultaneously with CB[7] and HSA allowing the possibility to compare the photoactivity of a broad range of AO⁺ species. Therefore, we set out to investigate the photoactivity of the different complexes of AO⁺ and obtain further insights into the mechanism of action and ROS generation in the biosupramolecular complex. We compared the photoactivity of AO⁺ with TMPyP⁴⁺ and methylene blue (MB⁺), another well-known photosensitizer (scheme 1), which shined light on the importance of the ternary biosupramolecular complex for drug photoactivity. Our results show that photoactivity cannot be predicted solely from the photophysical parameters of the photosensitizers in solution and in the complex with CB[n] because the mode of interaction of the various components in the system with the protein needs to be known.



Scheme 1. Chemical structures of CB[n]s ($n = 7, 8$), AO⁺, TMPyP⁴⁺ and MB⁺.

Experimental

Chemicals

Cucurbit[n]uril (CB[n], $n=7,8$), acridine orange (AO⁺), tetra(1-methylpyridinium)porphyrin (TMPyP⁴⁺), bis(ciclopentadienil)

cobalt(III) hexafluorophosphate (Cob⁺), 9,10-anthracenediyl-bis(methylene)dimalonic acid (ABMA), human serum albumin (HSA), bovine serum albumin (BSA), sodium azide (NaN₃) and deuterium oxide (D₂O) were obtained from Sigma and used without further purification. Methylene blue (MB⁺) was obtained from Merck and was recrystallized from benzene/MeOH (3:1). Potassium ferricyanide (FeCy) was obtained from Merck and used without further purification.

Sample preparation

Stock solutions of the photoactive molecules (AO⁺, MB⁺ or TMPyP⁴⁺) were prepared in water to approximately 1 mM and the actual concentration was assessed using their molar extinction coefficients (AO⁺ $\epsilon_{492\text{ nm}} 6.2 \times 10^4 \text{ M}^{-1} \text{ cm}^{-1}$,⁵⁵ MB⁺ $\epsilon_{664\text{ nm}} 8.4 \times 10^4 \text{ M}^{-1} \text{ cm}^{-1}$,⁵⁶ TMPyP⁴⁺ $\epsilon_{422\text{ nm}} 2.3 \times 10^5 \text{ M}^{-1} \text{ cm}^{-1}$).⁵⁷ Stock phosphate buffer (PB) solutions were prepared by mixing 100 mM Na₂HPO₄ and NaH₂PO₄ solutions to achieve a pH of 7.0 (pHmeter Hanna HI2221). Albumin (HSA or BSA) stock solutions were prepared at a concentration of 0.5 mM in 10 mM PB pH 7.0. Stock solutions of CB[7] were prepared in water to approximately 1 mM. Saturated solutions of CB[8] were prepared in 10 mM PB pH 7.0 and filtrated. Both CB[n]s were titrated against a known concentration of Cob⁺ by UV-Vis spectroscopy.⁵⁸

Aliquots of the stock solutions of the photoactive molecules, CB[n], albumin and PB were mixed directly in a spectrophotometric cell and the volume was completed to 3.00 mL with water. Final concentrations were 5 μM for AO⁺ and TMPyP⁴⁺, 10 μM for MB⁺, 50 μM CB[7], 35 μM CB[8], 5 μM for BSA, 25 μM for HSA and 10 mM PB pH 7.0. For the samples in the presence of additives, FeCy was added to a final concentration of 1 mM and NaN₃ to 10 mM. D₂O-enriched solutions were prepared by diluting stock solutions in D₂O instead of water (>80% D₂O).

Irradiation set-up

Sample irradiation was carried out in custom-built PTI equipment working with a 150 W Xe lamp. The irradiation wavelength was selected with a monochromator (10 nm bandwidth). The sample was stirred and the temperature was kept at 25°C using a waterbath. All samples were irradiated at their absorption maxima. AO⁺ was irradiated at 492 nm in the absence of CB[n]s and at 485 nm or 465 nm in the presence of CB[7] or CB[8], respectively.⁵² The irradiance absorbed by the samples was the same within error and equal to $31 \pm 3 \text{ W m}^{-2}$ (YSI Kettering 65A radiometer). TMPyP⁴⁺ was irradiated at 422 nm both in the absence or presence of CB[n]s since the absorption maximum did not change upon complexation.⁵¹ MB⁺ was irradiated at 664 nm in the absence of CB[n]s and at 659 nm in the presence of CB[7].^{59, 60}

Measurements

Protein photo-oxidation was assessed by the loss in the tryptophan fluorescence exciting the samples at 295 nm and measuring the emission at 350 nm. Upon irradiation, the samples were measured every 5 min for a total of 30 min. The absorbance at 295 nm was constant throughout the

irradiation, and therefore no inner-filter correction was applied. For the sample in the presence of AO^+ and CB[7], additional experiments were performed in the absence and presence of FeCy, D_2O and NaN_3 . Photo-oxidation experiments were performed in triplicate ($\leq 3\%$ error).

Total peroxide formation and hydroperoxides were quantified by the FOX-2 method,^{61, 62} according to a published procedure.⁶³ Briefly, during the irradiation, samples were withdrawn every 5 min and mixed in a proportion of 1:10 with FOX reagent containing 150 μM xylenol orange and 250 μM $(\text{NH}_4)_2\text{Fe}(\text{SO}_4)_2$ in 25 mM sulfuric acid. The absorbance of the product was measured at 560 nm and compared to a standard curve made with H_2O_2 . The quantification of hydroperoxides was done in the presence of catalase. The experiments were performed at least three times ($\leq 10\%$ error).

Protein electrophoresis (SDS-PAGE) was performed to measure HSA fragmentation and cross-linking. A stacking gel of 3% acrylamide and a resolving gel of 8% acrylamide were used. The proteins were denatured by boiling the samples for 5 min in loading buffer containing 62.5 mM Tris buffer pH 6.8, 2% SDS, 10% glycerol, 100 mM de β -mercaptoethanol and traces of bromophenol blue. The running buffer contained 25 mM Tris pH 8.3, 400 mM glycine and 0.1% SDS, and the electrophoresis was performed at 50 V for 20 min and at 100 V for 60 min. Silver staining was used to develop the gels and the electrophoretic pattern was analyzed with GelMax Imager and Doc-It[®]LS software from UVP. The results of the electrophoresis were consistent for repeated samples and the analysis shown herein corresponds to a representative experiment.

Laser flash photolysis was used to measure triplet excited state lifetimes for AO^+ and its complex with CB[7]. The samples were excited using a 266 nm Nd:YAG laser (Quanta-Ray Lab 130-4, Spectra Physics) and the detection of the excited state was done by monitoring the changes in the absorbance of the samples using a Xe-arc lamp from Oriol.⁶⁴ The concentration of the samples was 5 μM ($A_{266\text{ nm}} \sim 0.2$) and the samples were degassed with nitrogen for at least 20 min before the measurements. Decays of the triplet excited state of AO^+ in the absence and presence of 50 μM CB[7] were measured at 550 nm,⁵⁵ and at least 10 decays were averaged. The decays were fit to a monoexponential function to obtain the triplet excited state lifetimes.

Singlet oxygen ($^1\text{O}_2$) was detected by the bleaching of ABMA (1.6 μM) by fluorescence emission (Ex 395 nm / Em 407 nm). It must be noted that fluorescence was used only for a relative estimation of the production of singlet oxygen by the different complexes. To determine $^1\text{O}_2$ quantum yields (Φ_Δ) we used a high concentration of ABMA (200 μM) to trap all $^1\text{O}_2$,⁶⁵ and then the rate of consumption of ABMA was determined by following the absorbance at 380 nm during the course of irradiation. The rate of ABMA bleaching observed for irradiated samples of AO^+ in the absence or presence of CB[n]s was compared to Eosin Y as a standard ($\Phi_\Delta = 0.50$)⁶⁶. The absorbance of Eosin Y at the irradiation wavelength was matched to that of AO^+ species. The Φ_Δ was calculated from

the slopes of first-order plots as shown in equation 1.⁶⁷ Measurements were performed in triplicate.

$$\frac{\Phi_{\Delta\text{ sample}}}{\Phi_{\Delta\text{ standard}}} = \frac{(-d \ln A/dt)_{\text{sample}}}{(-d \ln A/dt)_{\text{standard}}}$$

Results and Discussion

Binding of AO^+ , MB^+ and TMPyP^{4+} to serum albumins, CB[n]s and ternary interactions

All the photoactive molecules used in this work bind to serum albumins with high affinity,^{50-52, 68-70} and the binding constants reported in the literature are summarized in table 1. We recently reported spectroscopic evidence for the binding of AO^+ close to Trp-214 in HSA, suggesting this molecule binds to Sudlow's site I.⁵² The data indicated mainly a 1:1 interaction, although some minor binding to other sites could not be discarded.⁵² A similar interaction was previously reported for AO^+ with BSA, although with lower affinity ($< 5 \times 10^3 \text{ M}^{-1}$).⁶⁹ The same type of binding has been reported for MB^+ with HSA, where electrostatic interactions played a major role in the stabilization of the complex.^{35, 70} The cationic porphyrin TMPyP^{4+} also binds to BSA through electrostatic interactions and the binding is favored at slightly basic pH.⁶⁸

Both AO^+ and MB^+ bind with a higher affinity to CB[7] compared to HSA (table 1), and form 1:1 inclusion complexes (denoted as $\text{AO}^+\text{@CB[7]}$ and $\text{MB}^+\text{@CB[7]}$).^{71, 72} On the other hand, TMPyP^{4+} binds to CB[7] with a lower affinity than with BSA (table 1).⁷³ This porphyrin can bind up to four CB[7] molecules, but the cooperative effect of sequential CB[7] binding to TMPyP^{4+} has not been analyzed.⁷³ The case is different for CB[8], which can bind up to two AO^+ or MB^+ molecules inside its cavity forming 2:1 complexes (denoted as $(\text{AO}^+)_2\text{@CB[8]}$ and $(\text{MB}^+)_2\text{@CB[8]}$). It must be noted that the formation of 1:1 and 2:1 complexes with CB[8] is stepwise, and their relative abundance depends on the concentration of the dye and the macrocycle.⁵² There is likely an interaction between TMPyP^{4+} and CB[8], but there are no reported binding constants.⁵¹

CB[8] can also bind two different molecules and form a 1:1:1 ternary complex, and this is particularly interesting when one of the components is a protein, as the one reported for TMPyP^{4+} and BSA, where a tryptophan residue in the protein is suggested to be included inside the CB[8] cavity together with one of TMPyP^{4+} pyridinium arms.⁵¹ The binding affinity of the porphyrin to BSA in the absence or presence of CB[8] is comparable (table 1). CB[7] can also induce the formation of a ternary complex with a protein, even though only one molecule is included in the cavity. For this, the molecule has to protrude out of the cavity of CB[7].^{50, 52} We observed this behavior for AO^+ in the presence of CB[7] and HSA, while no interactions were observed for the case of CB[8] probably due to its larger cavity size.⁵² The binding of the $\text{AO}^+\text{@CB[7]}$ complex to HSA occurs with lower affinity compared to free AO^+ (table 1). On the other hand, the inclusion complex between MB^+ and CB[7] does not interact with HSA,[†] which

suggests MB^+ is buried in the cavity of the macrocycle. This point is discussed in more detail later on.

Effect of $\text{CB}[n]$ s on protein photo-oxidation mediated by AO^+

The effect of the encapsulation of AO^+ into $\text{CB}[n]$ s and the formation of a ternary complex with HSA was investigated by irradiating different AO^+ /HSA samples in the absence or presence of either $\text{CB}[7]$ or $\text{CB}[8]$. Photo-oxidation of the tryptophan residue in HSA was followed by fluorescence emission. It is important to note that both free and protein-

bound species are present in the solutions, so that the results have to be interpreted as overall effects considering the main species present. Based on the binding constants reported in table 1, we estimate that in the absence of $\text{CB}[n]$, about 81% of AO^+ is bound to HSA. In the presence of excess $\text{CB}[7]$, all AO^+ is bound to $\text{CB}[7]$ and about 44% of that complex interacts with HSA to form the ternary $\text{AO}^+@[\text{CB}[7]:\text{HSA}]$ complex.

Table 1. Binding constants (K) for AO^+ , MB^+ and TMPyP^{4+} with albumins (HSA or BSA), $\text{CB}[n]$ ($n = 7,8$) and protein- $\text{CB}[n]$ interactions.

	$K_{\text{Albumin}} / \text{M}^{-1}$	$K_{\text{CB}[7] 1:1} / \text{M}^{-1}$	$K_{\text{CB}[8] 2:1} / \text{M}^{-2}$	$K_{\text{Ternary } 1:1:1} / \text{M}^{-1}$
AO^+	^a $(2.0 \pm 0.5) \times 10^5$ (HSA)	^a $(3 \pm 1) \times 10^6$	^a $(4 \pm 1) \times 10^{14}$	^a $(3.5 \pm 0.8) \times 10^4$ (HSA- $\text{CB}[7]$)
MB^+	^b $(1.5 \pm 0.2) \times 10^5$ (HSA) ^c $(4.06 \pm 0.04) \times 10^4$ (HSA)	^d $(1.3 \pm 0.3) \times 10^7$	^d $(1.1 \pm 0.5) \times 10^{16}$	-
TMPyP^{4+}	^e 7.3×10^5 (BSA) ^f 1.35×10^5 (BSA)	^g 8.2×10^4	-	^f 4.30×10^5 (BSA- $\text{CB}[8]$)

^aFrom reference ⁵² in 10 mM PB pH 7.0. ^bFrom reference ³⁵ in 100 mM PBS pH 7.4. ^cFrom reference ⁷⁰ in 50 mM Tris-HCl buffer pH 7.4. ^dFrom reference ⁷¹ in water pH 5.5. ^eFrom reference ⁶⁸ in 20 mM PB pH 5.0 at low HSA concentration; errors not reported. ^fFrom reference ⁵¹ in 5 mM PB pH 7.0; errors not reported. ^gFrom reference ⁷³ in water pH 4.0; errors not reported.

On the other hand, in the presence of excess $\text{CB}[8]$, all AO^+ is bound to $\text{CB}[8]$. The highest photo-oxidation was achieved for the sample in the presence of $\text{CB}[7]$, followed by the sample in the absence of $\text{CB}[n]$ (figure 1), which implies an enhancing effect for $\text{CB}[7]$ on the photoactivity of AO^+ . Contrasting with $\text{CB}[7]$, irradiation of the sample in the presence of $\text{CB}[8]$ results in a significant decrease in photo-oxidation (figure 1). We recently reported the different reactivity of $\text{MB}^+@[\text{CB}[n]]$ complexes in the excited state, where we observed that the $\text{CB}[7]$ complex was more reactive than the $\text{CB}[8]$ complex against an oxidant.⁶⁰ The reason for this behavior was proposed to be due to a stabilization of the triplet excited state inside $\text{CB}[7]$ and significant quenching inside $\text{CB}[8]$.⁶⁰ We addressed the triplet excited state dynamics for AO^+ and other molecules later in the discussion.

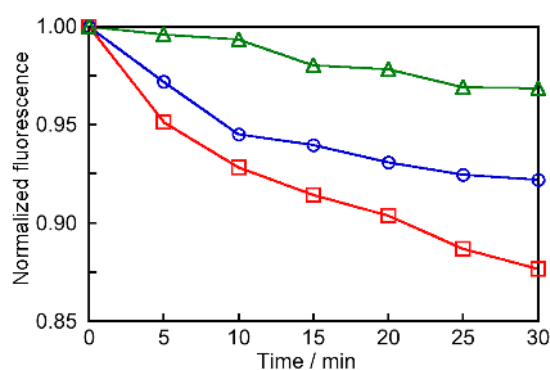


Figure 1. HSA photo-oxidation mediated by AO^+ in the absence of $\text{CB}[n]$ (blue circles) or in the presence of 50 μM $\text{CB}[7]$ (red squares) or 35 μM $\text{CB}[8]$ (green triangles). All samples in 10 mM PB pH 7.0 and irradiated at their absorption maxima.

During the course of HSA photo-oxidation, extensive photo-bleaching of AO^+ was observed for the sample in the presence of $\text{CB}[7]$ compared to the samples in the absence of $\text{CB}[n]$ or in

the presence of $\text{CB}[8]$, following the same trend as HSA photo-oxidation (figures S1, S2 and S3 in the ESI). This result was not expected since $\text{CB}[7]$ is reported to increase the photostability of several dyes,⁷⁴ which suggested a possible type I (electron-transfer) process for the $\text{AO}^+@[\text{CB}[7]]$ complex. Acridinium salts are known to be good electron donors in the excited state and are frequently used for photoorganocatalysis.⁷⁵ We further investigated the mechanism of photo-oxidation for the case where the highest photo-oxidation was observed, *i.e.* in the presence of $\text{CB}[7]$, by using additives such as the singlet oxygen scavenger NaN_3 , electron-acceptor FeCy , which interferes in photo-induced electron-transfer, and D_2O , which lengthens the lifetime of singlet oxygen by about 20 times. These compounds have been used in the past to study photo-sensitized oxidation.⁶³ As shown on figure 2, the addition of D_2O resulted in a minor increase in HSA photo-oxidation. If we compare this result with the effect of D_2O on the oxidation of HSA by MB^+ (a known type II photosensitizer), we can observe that the effect of D_2O is much larger for MB^+ (figure S4 in the ESI) compared to AO^+ . It must be noted that the isotopic effect of D_2O not only lengthens the singlet oxygen lifetime, but also lengthens the triplet excited state lifetime for MB^+ .⁷⁶ The addition of NaN_3 decreased the HSA photo-oxidation only to some extent, indicating that the amount of singlet oxygen that can be quenched by azide is little, and this agrees with the small enhancement observed with D_2O . The results discussed above point to a contribution of singlet oxygen in the photo-oxidation, but not likely as the only mechanism. On the other side, the addition of the electron-acceptor FeCy decreases the photo-oxidation of HSA, pointing to the participation of an electron-transfer mechanism. It must be noted that the magnitude of the effects of FeCy and NaN_3 are not comparable because the concentration of FeCy is much lower than azide in

order to avoid screening the absorption of light by the trapping agent.⁶³ In all cases, the effect of the additives on HSA photo-oxidation is smaller than expected for dyes free in solution,⁶³ which suggest that the photo-processes occur in the close vicinity of the protein, so that additives in solution do not have complete accessibility to inhibit protein photo-oxidation. The fact that the binding of AO^+ and $\text{AO}^+/\text{CB}[7]$ occurs near the tryptophan residue in HSA,⁵² is in agreement with a favorable type I photo-oxidation mechanism.

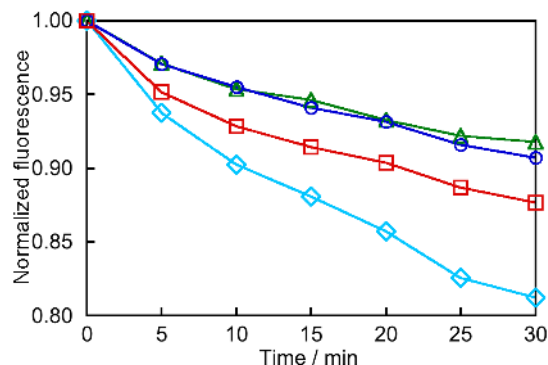


Figure 2. Effect of D_2O (cyan diamonds), FeCy (blue circles) and NaN_3 (green triangles) on HSA photo-oxidation in the presence of AO^+ and $50 \mu\text{M}$ $\text{CB}[7]$. The sample in the absence of additives (red squares) is shown for comparison. All samples in 10 mM PB pH 7.0 and irradiated at 485 nm .

Effect of $\text{CB}[n]$ s on the formation of peroxides mediated by AO^+

One of the most important reactive oxygen species generated as a consequence of type I and type II photo-processes are peroxides.⁷⁷ Peroxides can be formed as a consequence of type I mechanism when semireduced photosensitizers interact with oxygen^{78, 79} and/or from the dismutation of superoxide radical anion.⁸⁰ On the other hand, type II photo-processes also generate peroxides through the decomposition of singlet oxygen-generated endoperoxides.⁷⁷ We have shown before that hydrogen peroxide is the main species generated as a consequence of protein photo-oxidation mediated by electron-transfer mechanism, while protein hydroperoxides were not detected.⁶³ For AO^+ in the presence of $\text{CB}[7]$, the formation of peroxides is enhanced compared to the samples in the presence of $\text{CB}[8]$ or in the absence of any $\text{CB}[n]$ (figure 3). The enhancement in the generation of peroxides for the case of $\text{CB}[7]$ agrees with the increase in HSA photo-oxidation shown above (figure 1). By adding the enzyme catalase before the quantification of peroxides, which decomposes H_2O_2 much faster than protein hydroperoxides,⁶² we can estimate the amount of HSA hydroperoxides (HSA-OOH) and H_2O_2 in solution. We analyzed the generation of both types of peroxides for the sample that produced the highest amount of total peroxides, *i.e.* in the presence of $\text{CB}[7]$. As seen in the inset of figure 3, the generation of H_2O_2 is faster at short irradiation times but quickly levels off, while HSA-OOH increases in concentration over time, doubling the amount of H_2O_2 at long irradiation times. The fact that HSA-OOH are generated in a relatively high yield is important because these

species are long-lived in cells and can potentially enhance oxidative stress,⁶² which is beneficial for PDT applications.

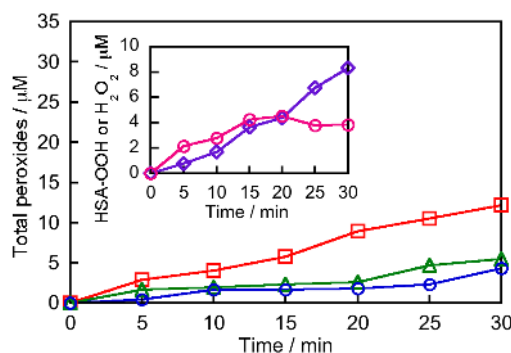


Figure 3. Peroxide generation during HSA photo-oxidation mediated by AO^+ in the absence of $\text{CB}[n]$ (blue circles) or in the presence of $50 \mu\text{M}$ $\text{CB}[7]$ (red squares) or $35 \mu\text{M}$ $\text{CB}[8]$ (green triangles). Inset: generation of HSA-OOH (purple diamonds) or H_2O_2 (pink circles) during HSA photo-oxidation in the presence of AO^+ and $\text{CB}[7]$. All samples in 10 mM PB pH 7.0 and irradiated at their absorption maxima.

Effect of $\text{CB}[n]$ s on HSA fragmentation mediated by AO^+

Protein cross-linking and fragmentation are common processes arising from photosensitization.⁸¹ A previous work reported the photocleavage of BSA induced by a ternary complex formed in the presence of TMPyP^{4+} and $\text{CB}[8]$.⁵¹ Therefore, we studied the fragmentation of HSA induced by different AO^+ species. As shown below, SDS-PAGE analysis of the samples irradiated in the presence of AO^+ alone or in combination with $\text{CB}[7]$ or $\text{CB}[8]$, reveals the occurrence of photo-induced fragmentation of HSA in all cases (figure 4). Control samples that were not irradiated, show the same electrophoretic pattern as the control sample containing only HSA, thus ruling out that either AO^+ or $\text{CB}[7]$ induce any modification in the protein. Control sample in the presence of $\text{CB}[8]$ shows some aggregation, which is seen as a diffuse band above the main band for HSA. $\text{CB}[8]$ -promoted aggregation has been reported before for the case of BSA,⁵¹ and could be related to the interaction of the macrocycle with hydrophobic aminoacids such as tryptophan and phenylalanine.^{82, 83} Some cross-linking could be observed above the band for HSA for the irradiated samples, although very minor. Fragmentation on the other hand, was estimated by densitometry to be between 10-16% higher in the irradiated samples compared to the control samples, being the highest when $\text{CB}[7]$ was present. The origin of the fragmentation could be related to the decomposition of HSA hydroperoxides, which are formed in considerable amounts as shown above. These HSA hydroperoxides are unstable and promote the formation of α -carbon centered radicals, which lead to protein cleavage.⁸¹

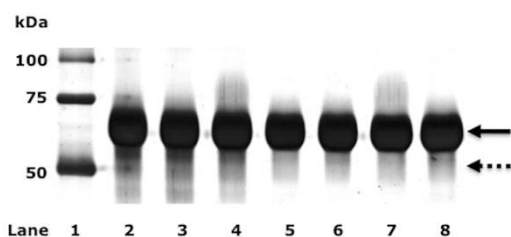


Figure 4. SDS-PAGE analysis of HSA irradiated for 30 min in the presence of the different AO^+ species and control samples without irradiation. The full arrow indicates the main band for HSA and the dotted arrow indicates fragmentation. Lane: (1) Molecular weight standard, (2) HSA irradiated with AO^+ , (3) HSA irradiated with AO^+ and CB[7], (4) HSA irradiated with AO^+ and CB[8], (5) control sample of HSA with AO^+ , (6) control sample of HSA with CB[7], (7) control sample of HSA with CB[8], and (8) control sample of HSA alone.

Comparison of the effect of CB[n]s on protein photo-oxidation mediated by TMPyP^{4+} and MB^+

We showed above that the overall photoactivity of AO^+ was enhanced in the presence of CB[7], *i.e.* higher HSA photo-oxidation, fragmentation and peroxide generation. This effect can be due to an overall enhancement of the photophysical and photochemical processes of AO^+ when forming an inclusion complex with CB[7], and/or due to the formation of a ternary complex with HSA, which would put the reacting species closer together facilitating their reaction. Therefore, it is useful to compare these results with the other photoactive molecules mentioned above: TMPyP^{4+} , which forms a ternary complex with BSA in the presence of CB[8] (and not CB[7]); and MB^+ , which forms inclusion complexes with both CB[7] and CB[8] (as does AO^+), but does not interact with HSA.

First, we studied BSA photo-oxidation in the presence of different species of TMPyP^{4+} . Figure 5 shows that BSA photo-oxidation is enhanced in the presence of TMPyP^{4+} and CB[8], when a ternary complex is formed, similar to the results observed for AO^+ . On the other hand, the sample in the presence of CB[7] shows the same level of photo-oxidation as in the absence of CB[7] (figure 5). This result is likely due to the fact that the binding of TMPyP^{4+} to BSA competes with the binding to CB[7] (see binding constants in table 1). It is noteworthy that TMPyP^{4+} acts mainly through singlet oxygen generation, while for AO^+ the electron-transfer mechanism is also important. In spite of this difference, the important point here is that in principle, the results obtained for AO^+ and TMPyP^{4+} are consistent, *i.e.* the highest photoactivity is observed for the samples where ternary interactions with the protein are favored. It is also interesting to note that both CB[7] and CB[8] can promote the association of the photoactive molecules to the protein and this depends on the structures of photoactive molecule as well as the protein.

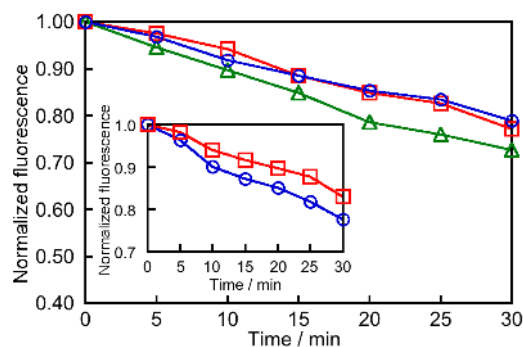


Figure 5. BSA photo-oxidation mediated by TMPyP^{4+} in the absence of CB[n] (blue circles) or in the presence of 50 μM CB[7] (red squares) or 35 μM CB[8] (green triangles). Inset: HSA photo-oxidation mediated by MB^+ in the absence (blue circles) or presence of CB[7] (red squares). All samples in 10 mM PB pH 7.0 and irradiated at their absorption maxima.

Another important comparison is between the photoactivity of AO^+ and MB^+ . The latter is structurally similar to AO^+ , it forms a 1:1 inclusion complex with CB[7] and it binds to HSA. However, there is no formation of a ternary complex with HSA. This is probably because unlike AO^+ , that protrudes out of the cavity of CB[7],^{84, 85} MB^+ is fully included in the cavity of CB[7] as previous studies suggest.^{59, 71} For MB^+ in the presence of CB[7], the photo-oxidation of HSA was lower compared to the sample in the absence of CB[7] (figure 5 inset). This trend is the opposite observed for HSA in the presence of AO^+ and CB[7], or BSA in the presence of TMPyP^{4+} and CB[8], which suggests the ternary interaction with the protein favor photo-oxidation, and the sole formation of an inclusion complex with CB[n] does not ensure the photoactivity is enhanced.

Effect of CB[n]s on triplet excited state lifetimes and singlet oxygen quantum yields for AO^+ , MB^+ and TMPyP^{4+}

Singlet oxygen generation by the different AO^+ species was detected by the loss in the fluorescence of water-soluble anthracene derivative ABMA.⁶⁵ It must be noted that $^1\text{O}_2$ detection is done in the absence of HSA, since proteins react with this species with high efficiency.^{81, 86} The complex of AO^+ with CB[7] produced the highest amount of $^1\text{O}_2$, followed by the CB[8] complex and free AO^+ (figure S5 in the ESI). Table 2 shows that the Φ_Δ for AO^+ increases significantly in the presence of CB[7]. This result agrees well with the trend observed in HSA photo-oxidation, fragmentation and peroxide generation described above. Surprisingly, CB[8] also increased the Φ_Δ compared to free AO^+ , in spite of the fact that a much lower photo-oxidation was observed for HSA in the presence of CB[8] (see figure 1). This is probably because protein photo-oxidation is measured as a loss of tryptophan fluorescence, when in fact several other aminoacids such as methionine, histidine, cysteine and tyrosine can also be photo-oxidized.⁸¹ In this sense, the location of the CB[n] complex within the protein where singlet oxygen is being generated can play an essential role in the protein photo-oxidation. While the CB[7] complex is thought to associate near the tryptophan residue (Trp-214), minor binding of the CB[8] complex away from the tryptophan

residue or the generation of singlet oxygen by the CB[8] complex in solution can lead to a lower photo-oxidation of this aminoacid residue.

If we compare these results with MB⁺ and TMPyP⁴⁺ there are important differences that need to be taken into account. The Φ_{Δ} for MB⁺ is slightly decreased in the CB[7] complex (table 2) due to a lower rate constant for oxygen quenching of the triplet excited state.⁵⁹ We observe the opposite effect for AO⁺, i.e. an enhancement of the Φ_{Δ} , which we believe is possible due to the fact that AO⁺ protrudes significantly out of the CB[7] cavity^{84, 85} compared to MB⁺, suggesting oxygen entry is not limited in this complex. This is the same effect observed for TMPyP⁴⁺, which is barely encapsulated into the CB[8] cavity.⁵¹

As for the reason of the enhancement in the Φ_{Δ} for AO⁺ in the presence of CB[8], it is anticipated that dimers in solution have greater intersystem crossing yields than the corresponding monomers at the expense of fluorescence emission.⁸⁷ However, inside CB[8] the behavior seems to depend on the molecule. For MB⁺, the Φ_{Δ} drops considerably (table 2). This result is consistent with a previous report of the decreased reactivity of the excited state of MB⁺ inside CB[8] against ferric ions (through electron-transfer) compared to the CB[7] complex.⁶⁰ The difference between the behavior of MB⁺ and AO⁺ could be related to a more favorable formation of the 2:1 complex in the case of MB⁺, which leads to self-quenching when MB⁺ is excited. This is not the case for AO⁺ since we reported previously a negative cooperativity for the binding of two AO⁺ molecules to CB[8].⁵² There is also the possibility that MB⁺ dimer forms a tighter complex inside CB[8] compared to AO⁺, restricting to a great extent the diffusion of oxygen.

Table 2. Triplet excited state lifetimes (τ_T) and ¹O₂ quantum yields (Φ_{Δ}) for photoactive molecules in the absence and presence of CB[7] or CB[8].

	No CB[n]		CB[7]		CB[8]	
	$\tau_T / \mu\text{s}$	Φ_{Δ}	$\tau_T / \mu\text{s}$	Φ_{Δ}	$\tau_T / \mu\text{s}$	Φ_{Δ}
AO ⁺	^a 160 ± 10	^a 0.18 ± 0.01	^a 210 ± 15	^a 0.50 ± 0.01	-	^a 0.31 ± 0.04
MB ⁺	^b 77 ± 5	^b 0.52	^b 150 ± 12	^b 0.44	-	^a ≤0.02
TMPyP ⁴⁺	^c 12.1	^c 0.74	-	-	^c 117.6	^{c,d} ≥0.90

^aThis work. ^bFrom references^{59, 76}; errors for Φ_{Δ} not reported. ^cFrom reference⁵¹; errors not reported. ^dLower limit determined in the presence of BSA. Singlet oxygen quantum yields determined in triplicate in air-equilibrated solutions. Triplet excited state lifetimes determined in nitrogen-saturated solutions.

Another important point in the comparison of the photoactivity of AO⁺, MB⁺ and TMPyP⁴⁺ are their triplet excited state lifetimes. As seen in table 2, the formation of a 1:1 inclusion complex for all the photosensitizers with CB[n]s lengthens the triplet excited state lifetime, which in the case of MB⁺ has been attributed to a slower non-radiative decay due to the restricted mobility imposed by the macrocycle.^{59, 76} Similar arguments have been given for the lengthening of the singlet excited state lifetime of several dyes inside CB[7] due to the low polarizability of its cavity.^{72, 74} For the case of TMPyP⁴⁺, the restriction of the movement of the porphyrin arms when

bound to CB[8] has been associated with longer triplet excited state lifetimes due to slower non-radiative deactivation.^{88, 89}

The lengthening of the triplet excited state lifetime does not necessarily reflect on a higher photoactivity. For example, the binding of TMPyP⁴⁺ to BSA also lengthens the triplet-excited state of the molecule, but the quenching of this state by oxygen is hindered within the protein, thus reducing its potential application in PDT.⁵⁷ This is the point where combining the protein as a vehicle with the inclusion into CB[n]s could have a strong impact.

Conclusions

The results show key points when considering the development of drug delivery systems using complex assemblies. Ternary complex formation between the photosensitizer, CB[n]s and the protein is a requirement for the enhancement of protein photo-oxidation. This requirement is independent of the photo-oxidation mechanism, type I or type II, because it was observed for AO⁺ and TMPyP⁴⁺.

Lengthening of the triplet excited state of the sensitizer due to CB[n] inclusion is not sufficient to enhance the quantum yield of singlet oxygen formation. The trends for this quantum yield suggest that the photosensitizer should not be buried in the cavity of the macrocycle, favoring the quenching by oxygen in the media. The protrusion of the guest is also a key point when favoring the interaction of the inclusion complex with the protein. In this regard, both CB[7] and CB[8] have shown to be capable of inducing this effect, but due to its greater solubility in water, the use of CB[7] is more promising in further biomedical applications.

Acknowledgements

This work was supported by CONICYT-FONDECYT (Grant 11121223) and at UVic by NSERC (RGPIN-121389-2012).

Notes and references

† No change in the anisotropy decays were observed for MB⁺ and CB[7] in the absence or presence of HSA. For more details on the technique see reference.⁵²

1. T. Reuters, *The Changing Role of Chemistry in Drug Discovery*, 2011.
2. T. M. Allen and P. R. Cullis, *Science*, 2004, **303**, 1818-1822.
3. W. J. Lambert, *Biopharm. Int.*, 2007, **20**, 32-39.
4. T. Lammers, *Int. J. Pharmaceut.*, 2013, **454**, 527-529.
5. C. Alvarez-Lorenzo and A. Concheiro, *Chem. Commun.*, 2014, **50**, 7743-7765.
6. F. Kratz, P. Senter and H. Steinhagen, *Drug Delivery in Oncology. From Basic Research to Cancer Therapy*, Wiley-VCH, 2012.
7. J. G. Moser, *Photodynamic tumor therapy: 2nd and 3rd generation photosensitizers*, Harwood Academic Publishers, 1998.

8. M. R. Hamblin and P. Mróz, *Advances in Photodynamic Therapy. Basic, Translational, and Clinical*, Artech House, 2008.
9. M. R. Detty, S. L. Gibson and S. J. Wagner, *J. Med. Chem.*, 2004, **47**, 3897-3915.
10. A. E. O'Connor, W. M. Gallagher and A. T. Byrne, *Photochem. Photobiol.*, 2009, **85**, 1053-1074.
11. H.-J. Schneider, *Supramolecular Systems in Biomedical Fields*, Royal Society of Chemistry, 2013.
12. A. R. Blaudszun, Q. Lian, M. Schnabel, B. Loretz, U. Steinfeld, H. H. Lee, G. Wenz, C. M. Lehr, M. Schneider and A. Philippi, *Int. J. Pharmaceut.*, 2014, **474**, 70-79.
13. A. C. Niehoff, A. Moosmann, J. Sobbing, A. Wiehe, D. Mulac, C. A. Wehe, O. Reifschneider, F. Blaske, S. Wagner, M. Sperling, H. von Briesen, K. Langer and U. Karst, *Metallomics*, 2014, **6**, 77-81.
14. S. Beyer, L. Xie, S. Grafe, V. Vogel, K. Dietrich, A. Wiehe, V. Albrecht, W. Mantele and M. G. Wacker, *Pharm. Res.*, 2015, **32**, 1714-1726.
15. L. Zhou, J. H. Liu, F. Ma, S. H. Wei, Y. Y. Feng, J. H. Zhou, B. Y. Yu and J. A. Shen, *Biomed. Microdevices*, 2010, **12**, 655-663.
16. Y. Svenskaya, B. Parakhonskiy, A. Haase, V. Atkin, E. Lukyanets, D. Gorin and R. Antolini, *Biophys. Chem.*, 2013, **182**, 11-15.
17. W. Miao, G. Shim, S. Lee, S. Lee, Y. S. Choe and Y. K. Oh, *Biomaterials*, 2013, **34**, 3402-3410.
18. C. S. Lee, W. Park, S. J. Park and K. Na, *Biomaterials*, 2013, **34**, 9227-9236.
19. C. E. Chen, L. Zhou, J. Geng, J. S. Ren and X. G. Qu, *Small*, 2013, **9**, 2793-2800.
20. M. Zamadar, G. Ghosh, A. Mahendran, M. Minnis, B. I. Kruff, A. Ghogare, D. Aebisher and A. Greer, *J. Am. Chem. Soc.*, 2011, **133**, 7882-7891.
21. D. Bartusik, D. Aebisher, G. Ghosh, M. Minnis and A. Greer, *J. Org. Chem.*, 2012, **77**, 4557-4565.
22. A. A. Ghogare, I. Rizvi, T. Hasan and A. Greer, *Photochem. Photobiol.*, 2014, **90**, 1119-1125.
23. F. Kratz, *J. Control. Release*, 2008, **132**, 171-183.
24. A. O. Elzoghby, W. M. Samy and N. A. Elgindy, *J. Control. Release*, 2012, **157**, 168-182.
25. F. Kratz, *J. Control. Release*, 2014, **190**, 331-336.
26. S. Curry, H. Mandelkew, P. Brick and N. Franks, *Nat. Struct. Biol.*, 1998, **5**, 827-835.
27. J. R. Simard, P. A. Zunszain, J. A. Hamilton and S. Curry, *J. Mol. Biol.*, 2006, **361**, 336-351.
28. G. Sudlow, D. J. Birkett and D. N. Wade, *Mol. Pharmacol.*, 1975, **11**, 824-832.
29. S. Wanwimolruk, D. J. Birkett and P. M. Brooks, *Mol. Pharmacol.*, 1983, **24**, 458-463.
30. I. Vayá, V. Lhiaubet-Vallet, M. C. Jiménez and M. A. Miranda, *Chem. Soc. Rev.*, 2014, **43**, 4102-4122.
31. S. Monti and I. Manet, *Chem. Soc. Rev.*, 2014, **43**, 4051-4067.
32. E. Alarcón, A. M. Edwards, A. Aspée, C. D. Borsarelli and E. A. Lissi, *Photochem. Photobiol. Sci.*, 2009, **8**, 933-943.
33. E. Alarcón, A. M. Edwards, A. M. García, M. Muñoz, A. Aspée, C. D. Borsarelli and E. A. Lissi, *Photochem. Photobiol. Sci.*, 2009, **8**, 255-263.
34. Y. Zhang and H. Gerner, *Photochem. Photobiol.*, 2009, **85**, 677-685.
35. E. Alarcón, A. M. Edwards, A. Aspée, F. E. Moran, C. D. Borsarelli, E. A. Lissi, D. Gonzalez-Nilo, H. Poblete and J. C. Scaiano, *Photochem. Photobiol. Sci.*, 2010, **9**, 93-102.
36. D. H. Macartney, *Isr. J. Chem.*, 2011, **51**, 600-615.
37. S. Walker, R. Oun, F. J. McInnes and N. J. Wheate, *Isr. J. Chem.*, 2011, **51**, 616-624.
38. N. Saleh, I. Ghosh and W. M. Nau, in *Supramolecular Systems in Biomedical Fields*, ed. H.-J. Schneider, Royal Society of Chemistry, 2013, pp. 164-212.
39. J. X. Zhang and P. X. Ma, *Adv. Drug Deliver. Rev.*, 2013, **65**, 1215-1233.
40. Y. H. Ko, I. Hwang, D.-W. Lee and K. Kim, *Isr. J. Chem.*, 2011, **51**, 506-514.
41. L. Cao, M. Šekutor, P. Y. Zavalij, K. Mlinarić-Majerski, R. Glaser and L. Isaacs, *Angew. Chem. Int. Ed.*, 2014, **53**, 988-993.
42. G. Hettiarachchi, D. Nguyen, J. Wu, D. Lucas, D. Ma, L. Isaacs and V. Briken, *PLoS ONE*, 2010, **5**, 10514.
43. V. D. Uzunova, C. Cullinane, K. Brix, W. M. Nau and A. I. Day, *Org. Biomol. Chem.*, 2010, **8**, 2037-2042.
44. R. Oun, R. S. Floriano, L. Isaacs, E. G. Rowan and N. J. Wheate, *Toxicol. Res.*, 2014, **3**, 447-455.
45. P. Montes-Navajas, M. González-Béjar, J. C. Scaiano and H. García, *Photochem. Photobiol. Sci.*, 2009, **8**, 1743-1747.
46. C. Márquez and W. M. Nau, *Angew. Chem. Int. Ed.*, 2001, **40**, 3155-3160.
47. C. Márquez, R. R. Hudgins and W. M. Nau, *J. Am. Chem. Soc.*, 2004, **126**, 5806-5816.
48. H. Yang, B. Yuan, X. Zhang and O. A. Scherman, *Acc. Chem. Res.*, 2014, **47**, 2106-2115.
49. M. E. Aliaga, L. Garcia-Rio, M. Pessêgo, R. Montecinos, D. Fuentealba, I. Uribe, M. Martin-Pastor and O. Garcia-Beltrán, *New J. Chem.*, 2015, **39**, 3084-3092.
50. A. C. Bhasikuttan, J. Mohanty, W. M. Nau and H. Pal, *Angew. Chem.*, 2007, **119**, 4198-4200.
51. W. Lei, G. Jiang, Q. Zhou, B. Zhang and X. Wang, *Phys. Chem. Chem. Phys.*, 2010, **12**, 13255-13260.
52. K. Scholtbach, I. Venegas, C. Bohne and D. Fuentealba, *Photochem. Photobiol. Sci.*, 2015, **14**, 842-852.
53. T. Matsubara, K. Kusuzaki, A. Matsumine, K. Shintani, H. Satonaka and A. Uchida, *Anticancer Res.*, 2006, **26**, 187-193.
54. K. Kusuzaki, H. Murata, T. Matsubara, H. Satonaka, T. Wakabayashi, A. Matsumine and A. Uchida, *In Vivo*, 2007, **21**, 205-214.
55. A. Kellmann, *Photochem. Photobiol.*, 1974, **20**, 103-108.
56. W. L. F. Armarego and C. L. L. Chai, *Purification of Laboratory Chemicals*, 6th ed., Elsevier, Burlington, 2009.
57. I. E. Borissevitch, T. T. Tominaga and C. C. Schmitt, *J. Photochem. Photobiol. A*, 1998, **114**, 201-207.
58. S. Yi and A. E. Kaifer, *J. Org. Chem.*, 2011, **76**, 10275-10278.
59. M. González-Béjar, P. Montes-Navajas, H. García and J. C. Scaiano, *Langmuir*, 2009, **25**, 10490-10494.
60. T. Fuenzalida and D. Fuentealba, *Photochem. Photobiol. Sci.*, 2015, **14**, 686-692.
61. C. Gay, J. Collins and J. M. Gebicki, *Anal. Biochem.*, 1999, **273**, 149-155.
62. P. E. Morgan, R. T. Dean and M. J. Davies, *Free Radic. Biol. Med.*, 2004, **36**, 484-496.
63. D. Fuentealba, B. Friguet and E. Silva, *Photochem. Photobiol.*, 2009, **85**, 185-194.
64. Y. Liao and C. Bohne, *J. Phys. Chem.*, 1996, **100**, 734-743.
65. N. A. Kuznetsova, N. S. Gretsova, O. A. Yuzhakova, V. M. Negrimovskii, O. L. Kaliya and E. A. Luk'yanets, *Russ. J. Gen. Chem.*, 2001, **71**, 36-41.
66. R. W. Redmond and J. N. Gamlin, *Photochem. Photobiol.*, 1999, **70**, 391-475.
67. F. Wilkinson, W. P. Helman and A. B. Ross, *J. Phys. Chem. Ref. Data*, 1993, **22**, 113-262.

68. I. E. Borissevitch, T. T. Tominaga, H. Imasato and M. Tabak, *J. Lumin.*, 1996, **69**, 65-76.
69. X.-Z. Feng, Z. Lin, L.-J. Yang, C. Wang and C.-L. Bai, *Talanta*, 1998, **47**, 1223-1229.
70. Y. J. Hu, W. Li, Y. Liu, J. X. Dong and S. S. Qu, *J. Pharmaceut. Biomed.*, 2005, **39**, 740-745.
71. P. Montes-Navajas, A. Corma and H. García, *Chem. Phys. Chem.*, 2008, **9**, 713-720.
72. M. Shaikh, J. Mohanty, P. K. Singh, W. M. Nau and H. Pal, *Photochem. Photobiol. Sci.*, 2008, **7**, 408-414.
73. J. Mohanty, A. C. Bhasikuttan, S. D. Choudhury and H. Pal, *J. Phys. Chem. B*, 2008, **112**, 10782-10785.
74. W. M. Nau and J. Mohanty, *Int. J. Photoenergy*, 2005, **7**, 133-141.
75. D. Ravelli, M. Fagnoni and A. Albini, *Chem. Soc. Rev.*, 2013, **42**, 97-113.
76. E. I. Alarcón, M. González-Béjar, P. Montes-Navajas, H. García, E. A. Lissi and J. C. Scaiano, *Photochem. Photobiol. Sci.*, 2012, **11**, 269-273.
77. J. Cadet and P. Di Mascio, in *The Chemistry of Peroxides*, ed. Z. Rappoport, John Wiley & Sons, Ltd, 2006, vol. 2.
78. E. Silva, R. Ugarte, A. Andrade and A. M. Edwards, *J. Photochem. Photobiol. B*, 1994, **23**, 43-48.
79. A. de la Rochette, E. Silva, I. Birlouez-Aragon, M. Mancini, A. M. Edwards and P. Morliere, *Photochem. Photobiol.*, 2000, **72**, 815-820.
80. I. B. Afanas'ev, *Superoxide Anion: Chemistry and Biological Implications*, CRC Press, 1991.
81. D. I. Pattison, A. S. Rahmanto and M. J. Davies, *Photochem. Photobiol. Sci.*, 2012, **11**, 38-53.
82. H. Cong, L. L. Tao, Y. H. Yu, F. Yang, Y. Du, S. F. Xue and Z. Tao, *Acta Chim. Sin.*, 2006, **64**, 989-996.
83. A. R. Urbach and V. Ramalingam, *Isr. J. Chem.*, 2011, **51**, 664-678.
84. J. Liu, N. Jiang, J. Ma and X. Du, *Eur. J. Org. Chem.*, 2009, 4931-4938.
85. M. F. Czar and R. A. Jockusch, *Chem. Phys. Chem.*, 2013, **14**, 1138-1148.
86. M. J. Davies, *Photochem. Photobiol. Sci.*, 2004, **3**, 17-25.
87. E. G. McRae and M. Kasha, *J. Chem. Phys.*, 1958, **28**, 721-722.
88. S. L. Deng, T. L. Chen, W. L. Chien and J. L. Hong, *J. Mater. Chem. C*, 2014, **2**, 651-659.
89. G. H. Ahmed, S. M. Aly, A. Usman, M. S. Eita, V. A. Melnikov and O. F. Mohammed, *Chem. Commun.*, 2015, **51**, 8010-8013.